

COASTAL OCEANOGRAPHY USING A SMALL AUV

Edgar An⁽¹⁾, Manhar R Dhanak^{*(1)}, Lynn K Shay⁽²⁾,

Samuel Smith⁽¹⁾ and John Van Leer⁽²⁾

⁽¹⁾Department of Ocean Engineering,

Florida Atlantic University, Boca Raton, Florida, 33431

⁽²⁾Division of Meteorology and Physical Oceanography
RSMAS, University of Miami, Miami, Fl 33149

Abstract

Bathymetry, current and CTD measurements in shallow waters on the continental shelf off the coast of Florida, using a small, mobile, autonomous underwater vehicle (AUV) platform equipped with a 1200kHz broad band ADCP, are described. Florida Atlantic University's AUV, *the Ocean Explorer*, which was used in the mission, is a 7ft long versatile, Gertler body which can perform pre-programmed underwater missions to a depth of 1000ft. At a speed of 1-2 m/s, it can perform missions over a period of several hours, collecting in-situ oceanographic data and storing it on an on-board data-logger. The vehicle may also carry a side-scan sonar or a small-scale custom turbulence measurement package or other instruments for subsidiary measurements. The versatility of the AUV allows measurement of oceanographic data over a substantial region, the motion of the platform being largely decoupled from that of the sea surface.

In the missions of Dec. 5 and 11, 1997, 'lawn-mower pattern' AUV surveys were conducted over 1 km² regions on the east coast of Florida, north of Fort Lauderdale, at depths of 7m and 3m respectively in a water column where depth ranged from 10 - 32m. During Dec. 5, the region was subjected to a cold front from the northwest. Local wind measurements show presence of up to 10m/s winds at temperatures of up to 10-15⁰ C below normal for the time of the year. The fixed ADCP indicates occurrence of significant internal wave activity in the region. The data collected using the mobile AUV is utilized to develop a map of the bottom topography and examine current, temperature and density variations in the context of the background information from the fixed systems. The work described here is a significant step in the development of an autonomous oceanographic sampling network, illustrating the versatility of an AUV platform. The data collected during the missions described will form part of a bank for information on the impact of a cold front on shallow sub-tropical waters. We expect to repeat the missions during other such fronts.

1. Introduction.

The variability of currents in the coastal ocean contains a broad spectrum of temporal and spatial scales that are driven by winds, tides and the intrusion of boundary currents such as the Florida Current. To examine this variability, a rational approach requires a suite of instruments capable of resolving turbulent and fine scales to mesoscale variations in the current field. Given these inherent sampling issues, a combination of platforms are required to resolve the variability in an adaptive sampling strategy based upon the current ocean and atmospheric forcing conditions.

* Corresponding Author

Conductivity and temperature at fixed locations may be monitored using moored chains of sensors (Luther et al, 1999, for example). For current measurement, acoustic Doppler current profilers (ADCP) are commonly used in various configurations. Thus, an upward-looking ADCP may be mounted on a fixed platform on the seabed (Prandle, 1995, Lueck and Lu, 1997) or be suspended from moorings at an intermediate depth (see Stramma et al., 1995) to remotely measure local current velocities in the water column. Several ADCP's may be employed in a string or grid pattern to provide synoptic spatial variations of currents in the region.

Alternately, downward-looking ADCP's have been mounted on the hull of a moving ship (Joyce, 1989, Saunders, 1995) to provide current velocity information over the region. In this configuration, the ship's gyrocompass measurements and its ground speed are required to determine the current velocities (Marmorino and Trump, 1984, Chapman et al., 1997). However, the ADCP profiler must be calibrated to determine the absolute velocity profile (sum of the barotropic and baroclinic components). Potential sources of errors in the resulting current profiles are instrument sensitivity, its alignment (Joyce, 1989) and accuracy in bottom tracking. The seawater properties, such as the conductivity and temperature variations with depth, are characterized through periodic CTD casts from ships (see Fratantoni and Johns, 1996, for example). Typically, the cost of such operations can be fairly significant.

Expendable Current Profilers (XCP) are used to measure the upper ocean current and temperature structure to 1500m water depth (Sanford, 1986). These are typically deployed from an aircraft (AXCP) and provide 3-dimensional synoptic snapshots of the upper ocean variability. They can be particularly useful in storms (see for example, Shay 1992, 1998c).

Synoptic information of the upper mixed layer, such as the surface seawater temperature, can be measured from a remote satellite. Surface currents may be measured using a HF Doppler radar. The latter is based on utilizing the fact that the backscatter from ocean surface waves has a wavelength of one-half the radar wavelength (Crombie, 1955, Shay et al., 1995, 1998a,b, 1999). Use of HF radar to provide real-time surface currents in a coastal environment is becoming increasingly popular.

Platforms in the form of towed bodies have also been used for CTD and small-scale turbulence measurements (Fleury and Lueck, 1991, for example). Long tether lines are required to ensure that the platforms are free from vibrations associated with the motion of the surface ships; such vibrations lie in the frequency range of interest of fine scale measurements and can significantly corrupt the latter.

Small, mobile, autonomous underwater vehicles (AUVs) have recently become available as stable and reliable platforms for oceanographic measurement instruments and for conducting continuous surveys of the water column in a region. A number of efforts are underway in developing such mobile measurement platforms with the ultimate aim of establishing them as

basic elements in an oceanographic sampling network (Curtin et al., 1993). Notable recent oceanographic applications of the AUVs include ones involving Massachusetts Institute of Technology's Odyssey (Bellingham and Willcox, 1996, Schmidt et al., 1996), Woods Hole Oceanographic Institution's Autonomous Benthic Explorer (Yoerger et al., 1997, 1999), the large diameter NSWV vehicle (Levine and Lueck, 1996, 1999), the Southampton Oceanographic Center's Autosub (Griffiths et al., 1998), Naval Postgraduate School's Phoenix (Riedel and Healy, 1999) and Florida Atlantic University's Ocean Explorer (Dhanak and Holappa, 1999). Of these, the NSWV vehicle and the Autosub are fairly large vehicles. The others may be classed as small AUVs. The small AUVs are fairly versatile and can be low cost both in terms of hardware and operations, the latter being partly due to the fact that the vehicles can be launched from small research vessels. An AUV has an advantage over a tethered vehicle in that it is uncoupled from the motion of a surface mother ship so that (i) it is free from low frequency vibrations transmitted down tether lines, which can influence certain in-situ measurements, and (ii) operations are possible in storms when surface ships may not be able to operate. Using such mobile platforms, bathymetry maps can be developed at a relatively low cost, compared with those developed using surface ships, and the submesoscale ($O(10\text{km})$) distributions of currents, temperature, salinity and water density can be determined. In particular, if used in conjunction with other measurement systems outlined above, the small AUVs offer the possibility of making four-dimensional space-time measurements in an affordable way, potentially during a storm when processes such as sediment transport and turbulent mixing occur with great intensity and are expected to induce major changes to the bed form and the water column.

The AUV platforms provide an attractive autonomous means of making bathymetric and hydrographic surveys of a water column. Traditionally these have been carried out with fixed, ship-mounted or tethered platforms (see Fratantoni and Johns, 1996). For example, echo sounder systems from ships (see for example, Bourillet et al., 1996) are used to develop bathymetry maps of the region. While measurements from an ADCP mounted on an AUV have to contend with sources of error similar to those from a moving surface ship described above, they may be less prone to alignment problems in the relatively calmer underwater conditions and may allow bottom-tracking at good resolution in water columns whose full depth is out of range of a surface-ship mounted ADCP. Typically, in the absence of these errors, high-resolution current profiles can be acquired using presently available ADCPs over relatively short horizontal scales to examine fine scale variability across coastal fronts and eddies where considerable shears may occur due to differing water masses. Ideally, AUV based measurements compliment the fixed, the surface-ship based and ADCP measurements. In particular, they would work best if synoptic background information were available.

Here, the use of the *Ocean Explorer (OEX)* series autonomous underwater vehicles, built at Florida Atlantic University, as a platform for ADCP and CTD measurements is described.

The platform was used to survey two adjacent regions off the east coast of Florida during winter of 1997. The *OEX* and its instrument payload are described in section 2. Experimental missions of Dec. 5 and 11, 1997 on the east coast of Florida and measurements from a fixed upward-looking ADCP in the vicinity as well as prevailing atmospheric conditions from two NOAA C-MAN buoys are described in section 3.

2. The Ocean EXplorer Series Vehicle.

An *OEX* series AUV (Smith et al., 1995), is typically 2.4m long (Figure 1) with a modified Gertler Series 58 Model 4154 fiber-glass hull of 0.53m maximum diameter and an interior framework made of high-density polyethylene (HDPE) and 6061-T6 aluminum. The *OEX* is designed to support multiple in-situ sensor payloads for performing search and mapping operations in coastal shallow-water environments. Its unique feature is a modular bayonet-mount interface between its payload and tail-section, allowing easy switching between payloads. The 1.2m tail-section houses navigation, control and propulsion components whereas a nominal 1.2m payload section, which may be extended to 2.4m, is dedicated to house mission-specific instruments. In air, the *OEX* weighs approximately 181kg, and is designed to be neutrally buoyant. Its maximum depth rating is 300m although, to date, most of the operations have been carried out in less than 150m water depths. The control surfaces are aft-mounted with a cruciform shape, and are replaceable with different fin sizes for different vehicle lengths and propulsion requirements. Each of these fins is driven by a brush less DC motor via a worm gear. In addition to the fins, the 3-blade, 18-inch propeller is based on a modified NACA 4412 section, and is driven by a brush less DC motor via a spur gear; in a recent development, the latter has been upgraded to a fully flooded motor with no gears. Using its on-board rechargeable NiCad batteries, which can provide up to approximately 2kWh total energy, the *OEX* can maintain a cruising speed of 3 knots (a speed range of 2-5 knots) for approximately 10 hours continuously between the recharge cycles.

For navigation and control, the aft section (see Figure 1) of the *OEX* houses 1) an ADCP (1.200Hz Navigator from RD Instruments) which measures altitude and vehicle velocity with respect to either the water column or ground as well as providing current profiles, 2) a Watson Block self-motion package which provides attitude and heading information, including Euler angles, tri-axial body rates and acceleration, 3) a differential GPS receiver unit, 4) RF Ethernet, 5) a Falmouth Scientific Instrument's micro-CTD 2 (see specifications in Table 1), rated at max depth of 500m, which provides conductivity, temperature and depth measurement and 6) a Motorola 68060 CPU with a VX Works operating system and 1 Gbyte disk storage capacity for logging significant amount of navigation and environmental data. The presence of the motors and the batteries in the tail section can contaminate compass measurement. Therefore, an auxiliary TCM2 Precision Navigation flux-gate compass mounted in the payload section, instead of the Watson Block, is utilized to provide heading information. The accuracy of vehicle positioning and navigation underwater depends

primarily on the TCM2 flux-gate compass and the onboard ADCP that provide heading and speed measurements respectively. For small AUVs, the interior magnetic signatures are usually significant and such errors must be characterized and compensated for. Typical procedures involve spinning the compass together with the vehicle, and building a deviation table for the compass given the existence of a compass rose or another independent heading reference that is more accurate. Prior to the experiments described here, a compass rose was used to build the deviation table, from which a maximum of approximately 3° overall heading error was inferred. That is, over a 1km long leg transect, an overall positioning error of approximately less than 50 m is expected.

The *OEX* carries out pre-programmed missions defined using ASCII text files that can be downloaded to it underwater via an Ethernet cable or remotely while at surface via RF connection, thereby increasing the operational efficiency. The AUV has several safety features that allow it to surface if unexpected difficulties arise during periods of active sampling.

Instrumentation

During the missions described herein, the AUV carried the downward-looking 1200kHz ADCP and a Falmouth Scientific Instruments (FSI) micro-CTD (see specifications below), rated at a maximum depth of 500m; since the work described here, the CTD package has been replaced with a FSI micro-CTD2. The CTD sensors were calibrated by FSI with the instrument mounted on a model of the hull section of the AUV. The locations of these instruments on the bottom of the AUV are shown in Figure 1. On the mission of Dec. 5, the ADCP operated in a mode, which allowed measurement of local water velocity at the first ADCP bin 2m beneath the ADCP at 2Hz and the AUV ground velocity at the same rate, the two measurements being taken in an interleaving sequence. On the mission of Dec. 11, the ADCP operated in a current profiling mode, measuring the velocity in the water column beneath it at 16 bins with a vertical resolution of 1m. Again, the current measurements were interleaved with bottom tracking measurements, both at a sampling rate of 2Hz as before.

To allow for GPS fixes, the *OEX* was programmed to surface periodically during its mission. The AUV location was also continuously tracked acoustically via an USBL transponder from the research vessel, the *FAU Oceanear R/V*; the research vessel was also used to launch and recover the AUV. During the missions, 113 different variables were recorded on the on-board computer, including current magnitude and direction at the vehicle location, vehicle depth and altitude, its position in latitude and longitude, and *in-situ* conductivity and temperature.

3. ADCP-CTD measurement missions along the East Coast of Florida

3.1 Site and flow description

In the Florida Straits, the Florida Current has maximum speeds of 1.5 to 1.7 m/s that intermittently intrudes over the shelf break along the Florida Keys. Lee et al. (1992) found a gyre circulation along the inshore edge of the Florida Current with scales of O (50 to 100 km) and a seasonal signal modulating biological activity. Submesoscale ocean features have also been observed with scales of 5 to 15 km and lifetimes of about 12 to 24 hours in this coastal ocean regime (Shay et al., 1998). As the current exits the Florida Straits and joins the Antilles Current, its transport increases to about 40 Sv (Schott et al., 1988). The Florida Current turns northward and follows the continental slope that eventually forms the Gulf Stream core off Cape Hatter as.

These larger mesoscale flows have been observed with various techniques over the previous few decades, yet little is known about the upper-ocean variability between the submesoscale to mesoscale. Submesoscale ocean flows interact with mesoscale features as well as with the tides, winds, and waves, and are accentuated in regions where the bottom topography changes abruptly (i.e. shelf break). In particular, the Florida Current is generally located closest to the coast just off of Fort Lauderdale. Given the relatively small-scales embedded within this current, the spatial evolution of these flows and their relationships to surface processes have remained to a large extent unresolved due to inherent sampling issues.

The two missions involved surveying a 1km square region off the coast of Fort Lauderdale, on the edge of the Gulf Stream, where the water depth varies between 12m and 36m. The surveyed region lies between the second and third of the shallow long shore reefs found on the east coast of South Florida (see Figure 1b). The mission of Dec. 5, 1997 was carried out at the location approximately $26^{\circ} 9.18'N$, $80^{\circ} 4.61'W$, while that of Dec. 11, 1997 was carried out slightly south of this location, at approximately $26^{\circ} 8.01'N$, $80^{\circ} 4.8'W$, portions of the two regions overlapping. In this coastal region, currents are frequently induced by large eddies which spin off the Gulf Stream and during winter, the region is frequently subjected to cold fronts when winds of highly variable speeds and with temperatures $10^{\circ}C$ or more below ambient blow offshore from the northwest and are favorable to upwelling. Available background information recorded by NOAA's C-MAN buoys north and south of the region during the mission is shown in Figure 2. Station LKWF1 is at Lake Worth ($26^{\circ} 37'N$, $80^{\circ} 2'W$) about 51 km north, while station FWYF1 is at Fowey Rocks ($25^{\circ} 35'N$, $80^{\circ} 6'W$), about 63 km south of the surveyed regions. The wind speed, air and water temperature and the atmospheric pressure at the two stations during the period Dec. 1 - 12, 1997 are shown in Figure 2 a - d respectively; the air temperature, wind speed and barometric pressure are monitored respectively at heights 13.4m, 13.7m, 6m above mean sea level at LKWF1 and at 11m, 43.9m and 29.3m above sea level at FWYF1 (NOAA, 1998). The water temperature

recorded at the two sites over the period is shown in Figure 2e. The arrows in Figures 2a and 2b point in the direction the wind is blowing *to*, positive values implying blowing northwards (contrary to meteorological convention).

The prevailing winds in the region are generally from the south. However, as we can see from Figure 2, during the cold front of Dec. 5 - 9, 1997, the region was subjected to cold northwest winds at maximum speeds varying between 6 and 10 m/s, higher speeds occurring at FWYF1. It may be noted that the variation in wind direction is fairly consistent between the two stations even though approximately 114km separate them. The air temperatures drop by as much as 10⁰C at FWYF1 and by 15⁰C at LKWF1 during the spell. As may be expected, the water temperature at the northern station is generally cooler. During the cold front, it drops by about 2⁰C at LKWF1 and by about 1⁰C at FWYF1. The variation in air pressure at the two sites is markedly similar.

3.2 Background Ocean Conditions

Background current profiles were recorded by a moored, bottom-mounted, 150kHz EDO Acoustics Harbor Surveillance Current Profiler (HSCP) located at 26⁰ 5.7355'N, 80⁰ 5.2263'W near Port Everglades in Fort Lauderdale (see Figure 1b). The HSCP records velocity, at a time interval of 7.5 min., in 35 0.5m bins. A subset of these measurements, encompassing 23 days of observations, were used here to document the background ocean conditions for the AUV missions of Dec. 5 1997 (YD 339) and Dec. 11 1997 (YD 345); unfortunately, the HSCP malfunctioned on the latter date so that moored current profile data are not available for that date. In the analysis of the HSCP data, measurements above a water depth of 2 m were not used since the transducer angles may not have been optimal to resolve near-surface currents (Johns, 1988). The time series of the north and east components of the current at the 8.8m bin are respectively shown in Figure 2f and 2g for comparison with the currents measured by the AUV at a depth of 9m. Along-shelf currents in the range 0 - 0.8 m/s are observed in the figure over the range of the time series shown, the directions of the currents, interestingly, being not well correlated with that of the wind direction in Figures 2a or b. Backscattered acoustic signals were ensemble-averaged to form a profiler time series at 0.5m vertical intervals every 7.5 min. starting at 2 m and ending at 18 m depth. Around Julian Days 331 and 344, large amplitude fluctuations of period between 10 -15 hrs are apparent in the north (along-shelf) component of velocity. These are, however, suppressed between Julian Days 337 and 341 and are replaced by more rapid oscillations of apparent period of approximately 2 1/2 hours. Similar fluctuations are observed in the east (cross-shelf) component of velocity. The time series for other neighboring bins all collapse fairly well onto the one shown in the figures. The time series from the HSCP are described in detail below.

Low-Frequency Flows

To illustrate the observed current structure variability at the HSCP mooring, the profiler time series was low-pass filtered using a Lanczos-squared window with half power at 48 h (hereafter referred to as subinertial flows). These time series captured an episode of the Florida Current moving over the shallow water HSCP mooring (Fig. 3a). During this period, the northward current approached 40 cm s^{-1} , which occurred during the Dec. 5. AUV trial. As observed during the OPRC-2 experiment along the Florida Keys, the core of Florida Current has a maximum of $150\text{-}160 \text{ cm s}^{-1}$ (Shay et al., 1998a). However, most of the record indicates a coastal current with maximum speeds of about 20 cm s^{-1} directed towards the south. These low frequency flow events were barotropic, consistent with the notion that the shallow coastal ocean circulation is well-mixed.

Tidal Currents

The 23-d of ADCP measurements allows for the analysis of the tidal currents in the semidiurnal band (M_2) and the diurnal band (K_1). These two constituents seemingly dominate the current records inshore of the Florida Current, and are well resolved by the HSCP. From the HSCP data, the magnitude of the near-surface (4 m) tidal current speeds ($\sqrt{u^2+v^2}$, where u and v respectively refer to north (along-shore) and east (cross-shelf) components of the current velocity) for the semidiurnal (M_2) and diurnal (K_1) constituents were about 4 to 6 cm s^{-1} , respectively. In the cross-shelf direction, the phases for the current reversed direction below 6 m for the K_1 constituent, whereas the phase for the M_2 constituent was nearly constant. However, the amplitudes of the tidal currents in the cross-shelf directions were relatively weak of about 1 cm s^{-1} . Clearly the more energetic velocity components were in the along-shelf direction with amplitudes of 4 to 6 cm s^{-1} . In these components, the phases remained relatively constant with depth, ranging from 32° to 64° and -28° to -36° for the diurnal and semidiurnal constituents, respectively. Notice that the variance in the cross-shelf direction was a factor of 10 to 20 times less than in the along-shelf direction. The maximum current variance occurred at a depth of 6 m with an along-shelf variance of $731 \text{ cm}^2 \text{ s}^{-2}$. The explained variance of the observed tidal current variations u_0 by the m tidal components ($\sum_{p=1}^m u_p$) was determined from the expression:

$$1 - \frac{\sum_{i=1}^n \left\{ u_0 - \sum_{p=1}^m u_p \right\}^2}{\sum_{i=1}^n u_0^2}$$

where n is the number of data points (4407) and m represents the number of tidal constituents (2) as per Table 2. Tidal currents explained 3 to 7% of the observed current variance, which is consistent with upper ocean tidal currents found at the ADCP mooring along the Florida Keys (Shay et al., 1998a).

Other flows that are apparent in the records are 3-4 h period oscillations; these were isolated through high-pass filtering of the detided current records at 8 h using a Lanczos-squared window (Fig. 3b). In the along-shelf current component, these oscillations ranged from $\pm 25 \text{ cm s}^{-1}$, and on YD 339, these currents decreased to about 10 cm s^{-1} . By contrast, the cross-shelf component was considerably weaker with amplitudes ranging from $\pm 10 \text{ cm s}^{-1}$. Further, these oscillations were depth-independent as in the low frequency and tidal flows. While it has been shown that barotropic signals can exist within the internal wave band, it is unclear whether these oscillations were due to the surface boundary layer dynamics (Shay and Chang, 1997). The wind records shown in Fig. 2a,b indicated the passage of an atmospheric front over a few hours at both sites on YD 335. However, the tidal time series indicated a general decrease starting on YD 334 and by the time of the AUV measurements, tidal currents were 5 cm/s . By contrast, these higher-frequency motions of about 15 to 20 cm/s were excited by the winds on YD 335 and gradually decreased to about 10 cm/s during the AUV mission. Thus, the wind rather than the tide played an important role in the excitation of these motions that had periods significantly less than the local inertial period of 27 h.

4. AUV-Based Measurements

4.1 Mission of 12/05/97

The period of operation of this mission is marked on Figure 2 by the first set of vertical bars. The wind speed of $5 - 9 \text{ m/s}$ recorded at the C-MAN stations is consistent with the observation of a cold wind from the northwest in the region during the mission. In order to survey the area, the AUV traveled repeatedly along an “east-west lawn mower pattern” path at a pre-programmed depth of 7m , surfacing twice to obtain GPS fixes. The path comprised a total of seven east-west legs traversed in about 3 hours at an average speed of 1 m/s .

The instantaneous position of the vehicle in terms of its latitude, longitude and depth is shown in Figures 4a-d. The AUV started out at the northern boundary of the region, moved south and then traveled repeatedly along an east-west "lawn mower pattern" path at a pre-programmed depth of 7m , surfacing twice to obtain GPS fixes. The lengths of the long and the short legs of the pattern were chosen to be 1km and 200m respectively. The seven legs of the AUV path can be discerned from Figures 4b and 4d and the times when the AUV surfaces are clearly apparent from Figure 4c. During part of the sixth leg, approximately during 21:52 - 22:01 hrs GMT, the AUV got caught in an abandoned line and strayed from its programmed path. This section of the sixth leg is therefore excluded from the analysis below.

The instantaneous water depth as a function of latitude and longitude during the seven legs is shown in Figure 5. The bathymetry shown is obtained through measurement of vehicle depth using the pressure sensor in the onboard CTD package (see Table 1 for accuracy) and

the measurement of the vehicle altitude using the 1200 kHz ADCP. The latter measures this as well as the vehicle speed both over water and ground. The information from the four beams of the RDI ADCP is processed internally in the unit to provide the velocity and altitude data. In this mode of ADCP operation, the bathymetry resolution is limited by the accuracy in measurement of the vehicle’s altitude, depth and position over the traversed path and density of the vehicle track line in a given coverage area. Throughout the two missions, bottom track in the shallow water was maintained. At a given point along the vehicle path, the inferred water depth is estimated to be accurate within 1m while the geographical location of the point is estimated to be within 50m, taking account of navigational errors described in section 2. The information in Figure 5 has been interpolated in Figure 6a to develop a bathymetry map of the surveyed region. While a bathymetry survey using a single ADCP does not quite meet the International Hydrographic Office’s standard, it does provide a low-cost means to characterize fairly accurate bathymetry maps in shallow water (see Table 1. for sensor specification). From Figure 6, the fairly flat, meandering “channel” between the reefs is clearly apparent and is consistent with the available bathymetry map from a 1962 US Coast and Geodetic Survey shown in Figure 6e. The accuracy in bathymetry measurement cannot be inferred through detailed comparison between Figures 6a and 6e as significant storm-related changes to bathymetry are possible since the USCG survey was conducted. However, the range of variation in bathymetry and the prominent features are evident in both maps.

Table 1. OEX Sensor Specification

Item	Accuracy	Resolution	Range
FSI CTD Conductivity Temperature Pressure	± 0.005 mmho $\pm 0.005^{\circ}\text{C}$ $\pm 0.15\%$ of full scale	0.0001mmho 0.001 $^{\circ}\text{C}$ 0.001dbar	0 to 65mmho -2 to 32 $^{\circ}\text{C}$ 0 to 50 bar
TCM2 Heading Roll Pitch	0.5 deg (rms) ± 0.2 deg ± 0.2 deg	deg deg 0.1 deg	360 deg 70 deg 70 deg
RDI ADCP Bottom track Water track Altitude	$\pm 0.2\%$ $\pm 0.2\%$ $\pm 1\%$	1mm/s 1mm/s 1cm	30m 20m 30m
ORE USBL	1 meter	N/A	1km

The recorded water temperature and salinity data from the on-board CTD package for the seven legs are plotted in Figures 7 and 8 against the instantaneous longitudinal position of the AUV. The specifications of the CTD package are given in Table 1, from which we can infer an error of less than 0.01 psu in salinity. The water temperature and salinity depicted in the figures exhibit greater variability between legs in the deeper (easterly) waters than nearer the

shore. The approximate mean temperature of 24.5°C at the near-shore position is consistent with the CMAN buoy data shown in Figure 2e. The difference between the minimum and maximum measured temperature is about 0.8°C . The data in Figure 8 suggest occurrence of horizontal salt intrusions at around 7m depth along the legs at intermediate longitudes. The mean value of salinity is 35.7 psu, the difference between the minimum and maximum values being about 0.45 psu. The associated density variations along the legs are shown in Figure 9 and the measurements are plotted on the TS diagram in Figure 10. The data are generally aligned with the 1024 kg/m^3 pycnocline, suggesting a region of instability and significant small-scale activity. The difference between maximum and minimum values of density is about 0.23 kg/m^3 . The information is used to generate, through interpolation, regional maps of the distribution of temperature, salinity and water density (Figure 6b-d) at 7m depth. It may be noted that these are not synoptic maps, rather they characterize the spatial distribution of the in-situ measurements during the mission. Temporal variations on the scale of mission duration or smaller cannot be resolved in such a survey. However, multiple AUVs may be utilized to minimize the influence of temporal variability. The maps suggest that warmer, more saline waters generally lie in the eastern part of the region that is closest to the Florida Current. A region of cold, relatively less saline and less dense water, protrudes into the surveyed region from the south. The small-scale variations in density are clearly apparent in Figure 6d.

For this mission, the ADCP was programmed to measure and record its velocity relative to ground and its velocity through the ambient water, but not to profile the velocity in the water column. The velocity through the water is measured at the first ADCP bin, 2m beneath the vehicle. Thus, with a vehicle depth of 7m, we can only determine local currents at a 9m depth. The variation in the horizontal components of the current over each leg, about the mean for each leg, is shown in Figure 11 and the data has been interpolated to show the regional current distribution in Figure 4d. The current map has been generated from the data obtained while the vehicle was at 7m depth. Taking account of the navigational accuracy discussed in section 2, the length of the legs and the bilinear interpolation used in developing Figure 4d, it is estimated that the error in the position of the current vector is less than 50 m and the error in current velocities are of the order indicated in Table 1. Please note that as in the case of the other maps (Figure 6b-d), the Figure 4d does not represent a synoptic view. Temporal variations in the current of the order of variations of $O(3\text{ hr})$ or smaller are not properly resolved. Use of multiple AUVs is expected to improve the resolution. The magnitude and direction of the current is consistent with that measured by the moored HSCP (Figure 2f, g). A detailed comparison between the AUV current measurements and the HSCP is given in Figure 4e. The AUV measurements shown in this figure have been averaged over 7.5 minute intervals, consistent with the available HSCP data. The magnitudes of the current, particularly the cross-shelf component, are of the right order, considering that the HSCP is

located around 5 km south of the surveyed region. While the mean current is generally northwards, the cross-shelf variations seen in Figure 11 suggest presence of large-scale eddies or horizontal shear layers.

4.2 Mission of 12/11/97

The period of operation of this mission is marked on Figure 2 by the second set of vertical bars. The southerly wind of around 5 - 7 m/s speed recorded at the C-MAN stations is consistent with the observation of a 10-15 knot wind from the south-southeast in the surveyed area. Waves of around 0.5m were observed in the area. The relation of the chosen site (B) for this mission to the mission of Dec. 5, 1997 (A), and the mode of survey are shown in Figure 12. Site B lies southwest of site A, which was surveyed on Dec. 5, 1997, the longitudinal position of the two sites overlapping somewhat. Site B is generally shallower than site A and the area covered is smaller than at site A. This time the AUV traveled back and forth along a north south "lawn mower pattern" path at a pre-programmed depth of 3m, surfacing twice to obtain GPS fixes. The path comprised several north-south legs, around 1km in length and separated by around 200m from neighboring legs, traversed in about 2.5 hours at an average speed of 1.3 m/s. The recorded CTD data was interpolated as before to obtain the local bathymetry and the distribution of temperature, salinity and density at a depth of 3m (Figure 13). The water depth generally increases from 10m to 15m with distance from the shore, although some cross-shelf ridges are apparent in the figure; the water depth is consistent with that at site A (Figure 6a). The bathymetry is consistent with the US Geological Survey of 1962 (Figure 6e) as before. The temperature distribution at the 3m depth has a mean of 24.71⁰C and a range of 0.1⁰C, the temperature increasing with distance from the shore while the salinity distribution at 3m has a mean of 36.1psu and a range of 0.14psu, the salinity generally decreasing with distance from the shore. The corresponding water density distribution has a mean of 1024.27 kg/m³ and a range of 0.12 kg/m³, the density decreasing with distance from the shore. The measurements imply that near-shore waters are cooler, more saline, and therefore denser, than off-shore waters although the differences are rather small. The water temperature is typical for the region during winter. It is not possible to make direct comparison of the temperature and salinity distributions between the two surveys in view of the differences in locations relative to the shore as well as in the survey depths. It may be noted, however, that in the region where the longitudinal positions overlap, although the mean water temperature at 3m depth on Dec 11, 1997 is generally the same as at 7m depth during the passage of the cold front on Dec 5, 1997, the water is more saline and therefore denser in the former case. Also evident is the reduction of small-scale variations such as in density seen in Figure 6d.

For this mission, the on-board 1200kHz ADCP was programmed to record the velocity profile of the flow beneath the vehicle at a bin spacing of 1m. The local current field at depth 5m, as interpolated from the ADCP measurement, is shown in Figure 12. The ADCP data

from 8 -14 bins, covering water depth of 5 - 17m, was interpolated to obtain current velocity transects along five north-south legs. Only bins that were free from any apparent contaminations from bottom reflections were utilized. The data for each bin was low-pass filtered with a cutoff at ~40m along shelf direction and resampled on an equally spaced grid. The east-west (cross shelf), north-south (along shelf) and downward velocity components are respectively plotted against instantaneous latitude position of the vehicle in Figures 14a-c. The cross shelf component is seen in Figure 14a to be generally shoreward, varying in magnitude between 0-10 m/s. The magnitude of the northward along shelf component in Figure 14b varies from a value of around 20 cm/s at the easternmost locations to -5 cm/s at the shallower, near shore locations. Thus the current direction apparently varied during the mission from north-northwest to southwest on approach to shore. It may be noted that the survey over the six consecutive legs shown in Figure 14 was carried out over a period of 86 minutes and the results are subject to time aliasing issues discussed below. The characteristics of the depth profiles for the locations away from the shore suggest that the flow there was driven by the presence of significant northbound winds depicted in Figure 2a,b. The mean value of the vertical component for each bin in Figure 14c has upward values below 2cm/s.

5. Discussion

A small AUV platform provides tether free, low operational cost method of surveying substantial regions of the water column, potentially during storms. The *OEX*-series AUV appears to be a good mobile platform in this category. Significant information about the bathymetry and spatial variability in the water column in a region can be identified with a few passes as in the missions described here. Refined information can be obtained through use of more, tighter, passes in a 'lawn-mower pattern'. Temporal variations on the scale of mission duration or smaller cannot be resolved in such a survey. The problem can, however, be reduced through use of multiple vehicles and conducting the survey in the presence of other fixed synoptic systems which can provide subsidiary background information about the temporal variability.

Recent studies (Shay et al. 1999) off the east coast of Florida utilized a shore-mounted OSCAR HF radar to provide surface current measurements while the *OEX* AUV made detailed measurements of current profiles, temperature and conductivity in the water column under the OSCAR grid. CTD and current measurements were also made from a ship. This latest work will result in unprecedented information about the mixed layer in waters influenced by the presence of the Florida Current.

The bathymetry data collected during the missions described here are consistent with the available hydrographic surveys of the region, illustrating the usefulness of the AUV. The currents measured by the onboard ADCP are also consistent with that measured by a nearby

moored ADCP. Further missions using the AUVs, in conjunction with other fixed systems, are planned in shallow waters off the east coast of Florida in order to further develop a comprehensive dataset to study active processes in the mixed layer during the passage of cold fronts over tropical waters. The coastal circulation in the area is dominated by the movement of the Florida Current over the shelf, by tidal currents, and by wind events, of the type described here, which may generate barotropic internal waves. While it is unclear whether the higher frequency motions observed in the moored HSCP data are solely internal waves, examining their behavior relative to the AUV measurements represents an important first step. Moreover, since the currents observed at the HSCP were generally barotropic, the comparisons with the AUV measurements on Dec. 5 at the 8-9 m level reflect the variability throughout the column, especially during vertically well-mixed conditions. In addition, vortices and spin-off eddies are often present in this area. Thus, subsequent experiments will have to be of sufficient duration to resolve the low frequency flows associated with these processes. In particular, AUV systems will work best in conjunction with fixed, ideally synoptic, measurements.

Acknowledgments: The work is supported by the Office of Naval Research through grants N00014-96-5023 and N00014-97-1-0672 (Program Manager: Dr Thomas Curtin). LKS and JVL acknowledge funding support from the Office of Naval Research through grant N00014-96-1101.

References

- Bellingham J. G. and Willcox J. S., 1996. Optimizing AUV Oceanographic Surveys, *1996 IEEE Symposium on Autonomous Underwater Vehicle Technology*, Monterey, 391-406.
- Bourillet JF, Edy C, Rambert F, Satra C, Loubrieu B. 1996. Swath Mapping System Processing: Bathymetry and Cartography. *Marine Geophysical Researches*, **18**, 487-506.
- Chapman, R. D., L. K. Shay, H. C. Graber, J. B. Edson, A. Karachintsev, C. L. Trump, and D. B. Ross, 1997: Intercomparison of HF radar and ship-based current measurements. *J. Geophys. Res.*, **102**, 18739-18,748.
- Crombie, D. D., 1955: Doppler spectrum of sea echo at 13.56 Mc s⁻¹. *Nature*, **175**, 681-682.
- Curtin, T., J. Bellingham, J. Catipovic, and D. Webb. 1993. Autonomous Oceanographic Sampling Networks. *Oceanography*, Vol.6, No.3, pp.86-94.
- Dhanak, M. R. and K Holappa. 1999. An Autonomous Ocean Turbulence Measurement Platform. *J. Atmos. Ocean. Tech.*, **16**, 1506 - 1518.
- Fleury, M. and R. G. Lueck. 1991. Fluxes across a thermohaline interface. *Deep-Sea Research*, **38**, 745-769.
- Fratantoni D. M, Johns W. E. 1996. A Deep-towed ADCP-CTD Instrument Package Developed For Abyssal Overflow Measurements In The Northeastern Caribbean Sea. *J. Atmos. Ocean. Tech.*, **13**, 680-687.
- Griffiths, G., N. Millard, S. Mcphail, P. Stevenson, J. Perett, M. Pebody, A. Webb. Towards Environmental Monitoring with the Autosub Autonomous Underwater Vehicle. 1998. *Underwater Technology Conference*, Tokyo, Japan, pp.121-125.

- Joyce, T. M., 1989: On In Situ "Calibration" of Shipboard ADCPs. *J. Atmos. Ocean. Tech.*, **6**, 169-172.
- Leaman, K. D., 1976: Observations of vertical polarization and energy flux of near-inertial waves. *J. Phys. Oceanogr.*, **6**, 894-908.
- Lee, T. N., C. Rooth, E. Williams, M. McGowan, A. F. Szmant, and M. E. Clarke, 1992: Influence of Florida Current, gyres, and wind-driven circulation on the transport of larvae and recruitment in the Florida Keys coral reefs. *Cont. Shelf Res.*, **12**, 971-1002.
- Levine E. R. and Lueck, R. G., 1996: Estuarine turbulence measurements with an autonomous underwater vehicle, *EOS, Trans. AGU*, 76, 3, OS79.
- Levine E. R. and Lueck, R. G., 1999: Turbulence Measurement from an Autonomous Underwater Vehicle, *J. Atmos. Ocean. Tech.* Vol. 16, pp. 1533-1544.
- Lueck RG, Lu YY. 1997. The Logarithmic Layer In A Tidal Channel. *Continental Shelf Research* **17**. 1785-1801.
- Marmorino, G. and C. Trump, 1994: A salinity front and a current rip near Cape Hatteras, U.S.A. *J. Geophys. Res.*, **99**, 7627-7638.
- Prandle D. 1993. Yearlong Measurements Of Flow-through The Dover Strait By Hf Radar And Acoustic Doppler Current Profilers (ADCP). *Oceanologica ACTA* **16** 457-468.
- Riedel, J.S., Healey, A.J. 1999. "Estimation of Directional Wave Spectra from an AUV" *Proceedings of 11th International Symposium on Unmanned Untethered Submersible Technology (UUST'99)*, August 22-25, 1999.
- Sanford, T. B., 1986: Recent improvements in ocean current measurement from motional electric fields. *Proceedings IEEE 3rd Working Conference on Current Measurement*. G. F. Apell and W. E. Woodward, eds., IEEE, New York, New York, 65-76.
- Saunders PM, King BA. 1995. Bottom Currents Derived From A Ship-borne ADCP On Woce Cruise A11 In The South-Atlantic. *Journal Of Physical Oceanography*. **25**. 329-347.
- Schmidt, H., J. G. Bellingham, M. Jhonson, D. Herold, D. M. Farmer, and R. Pawlowicz. Real-time Frontal Mapping With AUVs in a Coastal Environment. *Proc. MTS/IEEE Oceans'96*. Ft. Lauderdale, FL. 1094-1098.
- Schott, F., T. N. Lee, and R. Zantopp, 1988: Variability of the structure and transport of the Florida Current in the period range of days to seasonal. *J. Phys. Oceanogr.*, **18(9)**, 1209-1230.
- Shay, L. K., P. G. Black, A. J. Mariano, J. D. Hawkins and R. L. Elsberry, 1992: Upper ocean response to hurricane Gilbert. *J. Geophys. Res.* **92(12)**, 20, 227-20, 248.
- Shay, L. K., H. C. Graber, D. B. Ross and R. D. Chapman, 1995: Mesoscale surface current variability detected by HF radar. *J. Atmos. and Ocean. Tech.*, 12(4), Part 2, 881-900.
- Shay, L. K. and S. W. Chang, 1997: Free surface effects on the near-inertial ocean current response: a revisit. *J. Phys. Oceanogr.*, **27(1)**, 23-39.
- Shay, L. K., S. Lentz, H. C. Graber, and B. K. Haus, 1998a: Current structure variations detected by HF radar and vector measuring current meters. *J. Atmos. Ocean. Tech.*, 15, 237-256.
- Shay, L. K., T. N. Lee, E. J. Williams, H. C. Graber, and C. G. H. Rooth, 1998b: Observed submesoscale current structure detected by HF radar and an acoustic Doppler current profiler. *J. Geophys. Res.*, 103, 18,691-18,714.
- Shay, L. K., A. J. Mariano, S. D. Jacob, and E. H. Ryan, 1998c: Mean and near-inertial ocean current response to hurricane Gilbert. *J. Phys. Oceanogr.*, **28**, 858-889.

Shay, L. K., T. Cook, B. K. Haus, J. Martinez, H. Peters, A. J. Mariano, J. VanLeer, E. An, S. Smith, A. Soloviev, R. Weisberg, M. Luther., 2000. A Submesoscale Ring In The Coastal Ocean Detected By Very High Frequency Radar. Submitted to EOS.

Smith, S. M., K. Heeb, N. Frolund, T. Pantelakis, 1995. The Ocean Explorer AUV: A Modular Platform for Coastal Oceanography, *UUST*, Durham, New Hampshire, September, 1995.

Stramma L, Fischer J, Reppin J. 1995. The North Brazil Undercurrent *Deep-sea Research Part I-oceanographic Research Papers* **42**. 773-795.

Yoerger, D. R., A Bradley, B Walden. 1997. Scientific Survey with the Autonomous Benthic Explorer. *10th International Symposium UUST 97*, pp.41-49, Durham, New Hampshire.

Yoerger, D. R., A. Bradley, M-H Cormier, W B F Ryan, and B Walden. 1999. High Resolution Mapping of a Fast Spreading Mid-Ocean Ridge with the Autonomous Benthic Explorer. Proc. *11th UUST, AUSI*, Durham, NH, August 1999.

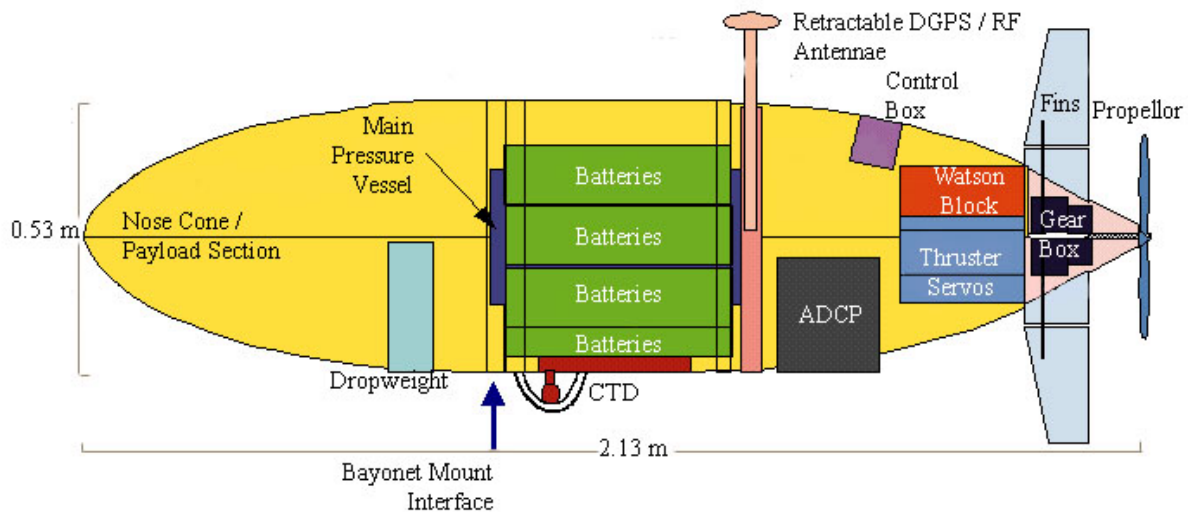


Figure 1. Schematics of the OEX-series AUV showing the location of the CTD and the ADCP

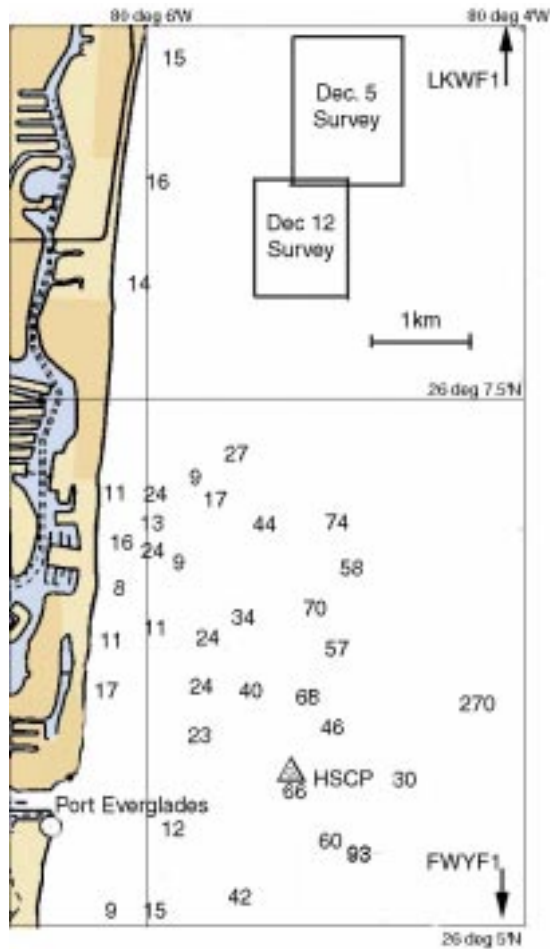


Figure 1b. Experimental site, showing the location of the surveyed regions and of the fixed HSCP current profiler. The soundings are in feet.

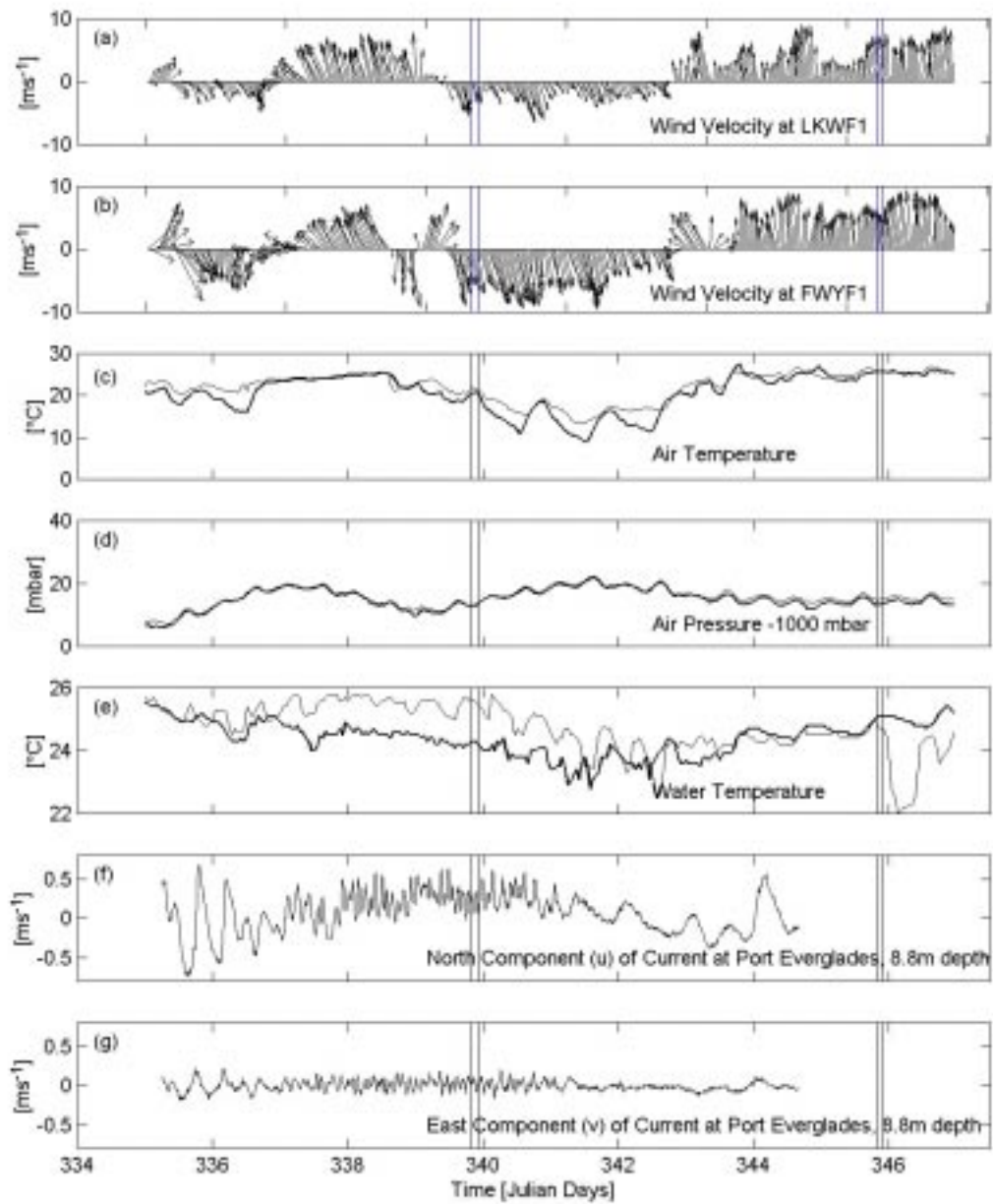


Figure 2. Meteorological (a-d) and water temperature data (e) recorded by CMAN buoys LKWF1 (thick line) and FWYF11 (thin line), located about 50 miles north and south of the site respectively, for 12/1/97 - 12/12/97. Raw current data from a fixed ADCP (HSCP) located 5km south of the region are also shown (f-g). The vertical bars mark times of AUV operations.

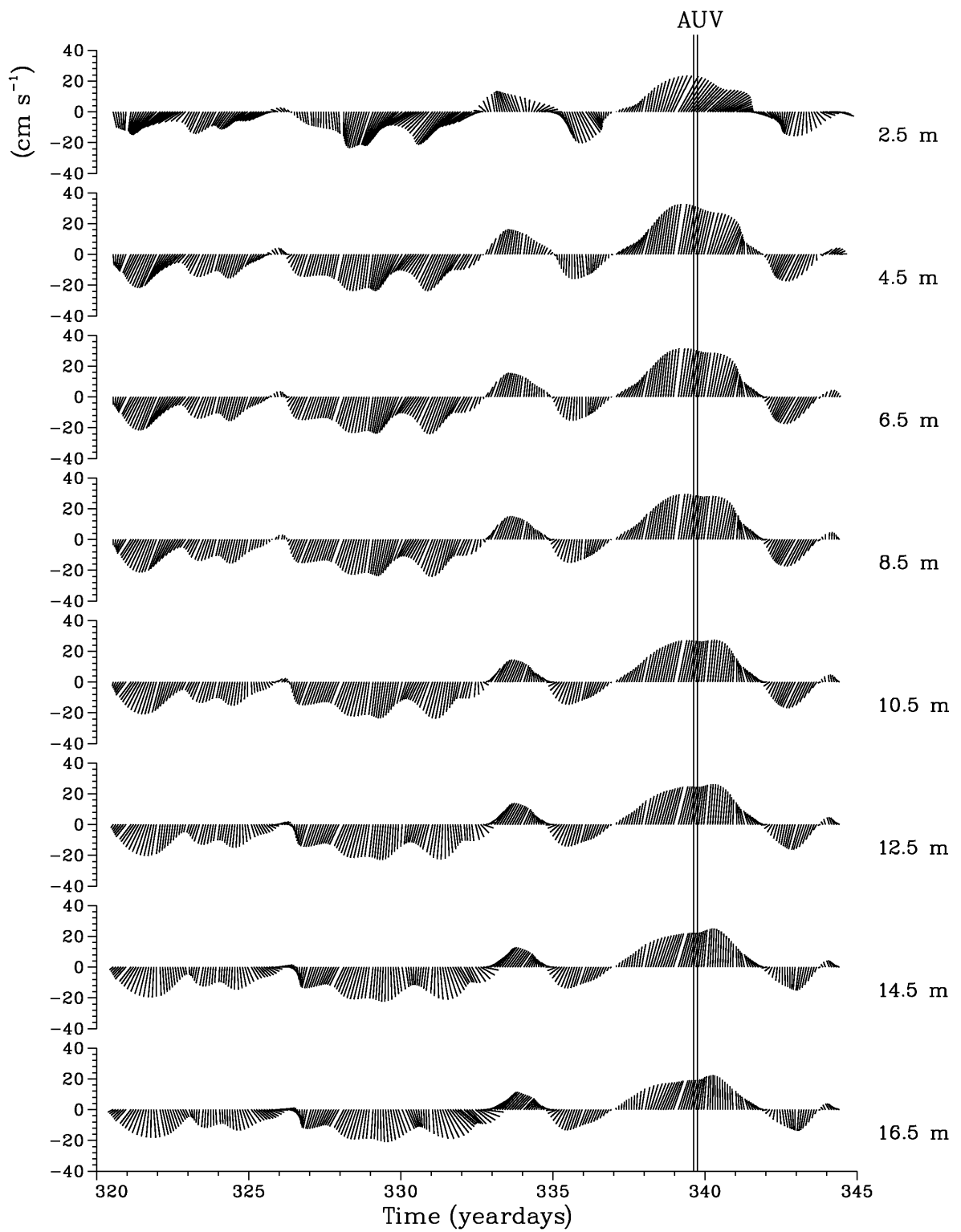


Figure 3a. Time series of 48-h low-pass filtered current records from the shallow-water ADCP the mouth of Port Everglades at selected depths throughout the water column.

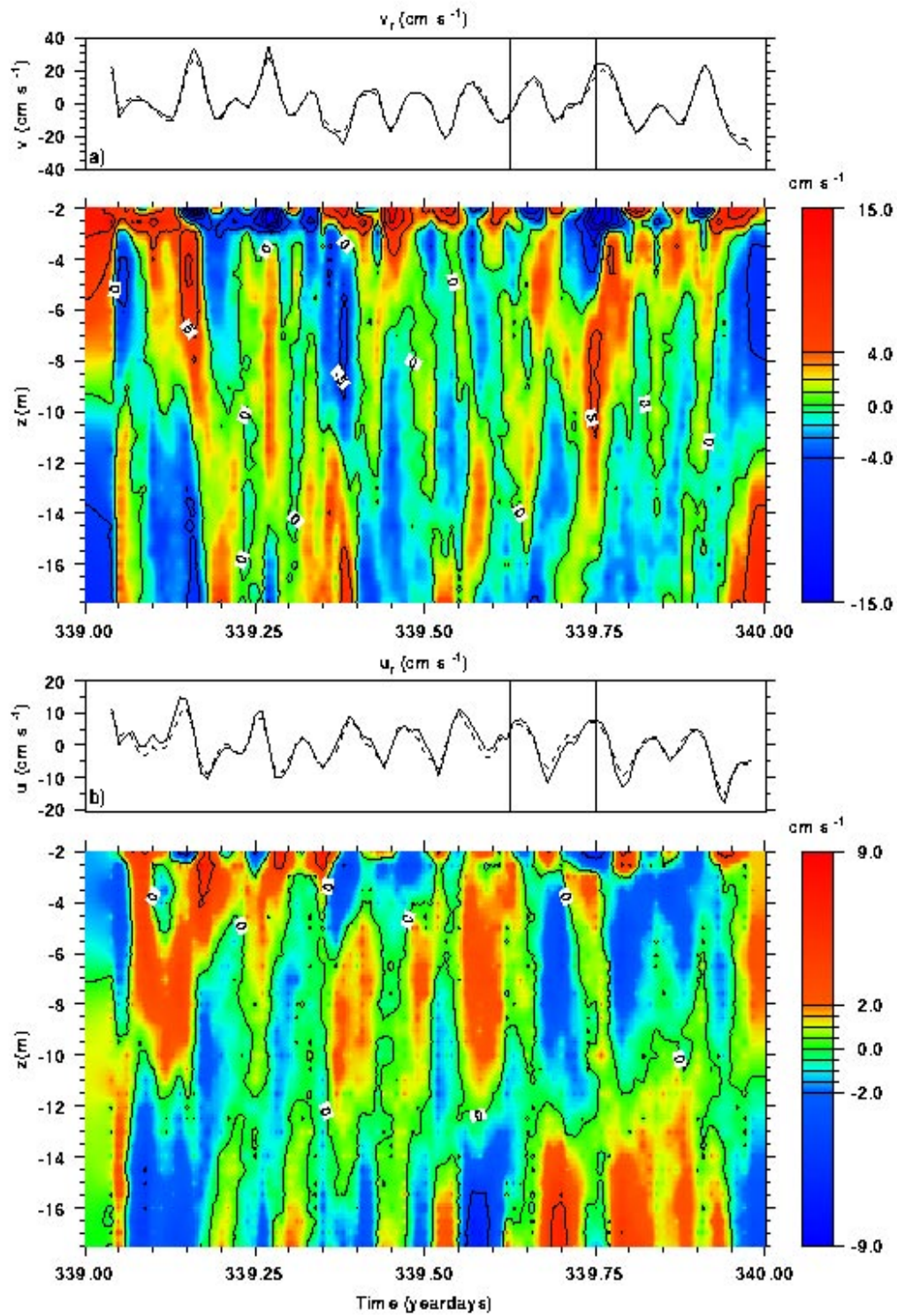


Figure 3b. 8-h high-pass filtered detided current profile contours from the shallow water, bottom-mounted ADCP (HSCP) for the (a) along-shelf and (b) cross-shelf components for Dec. 5, 1997. Upper panels represent the current at 7m and the depth-averaged current (dashed).

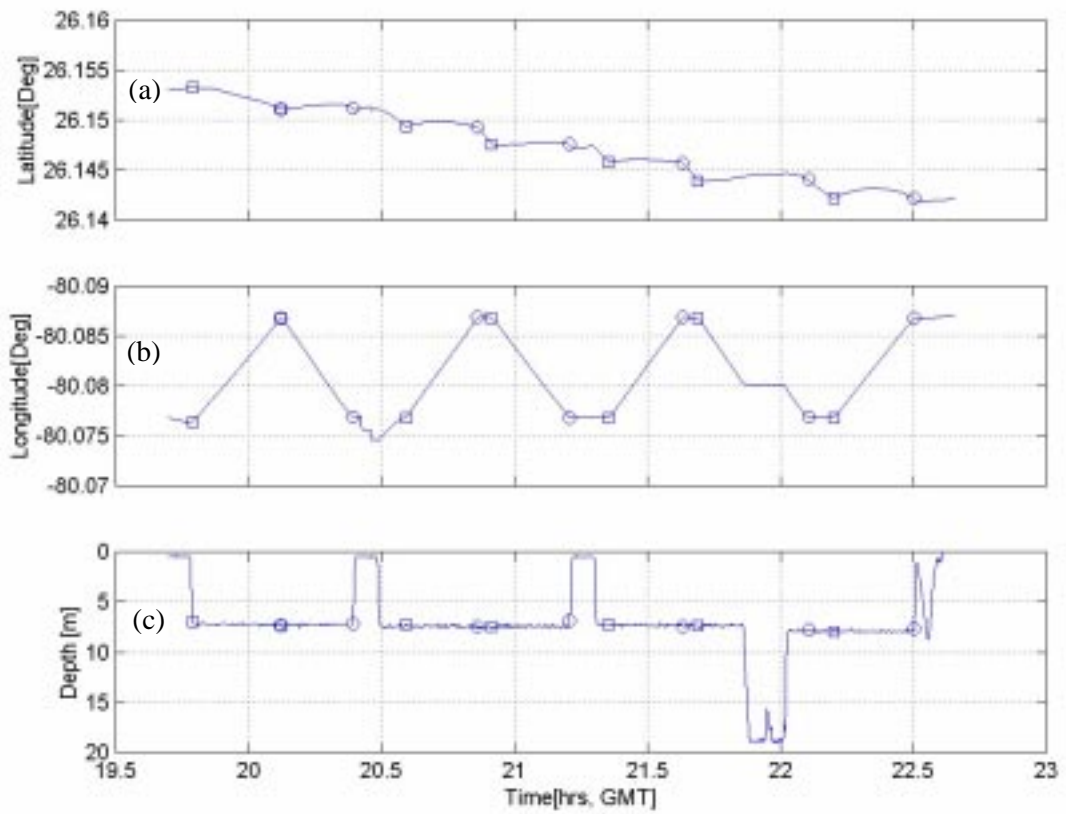


Figure 4a-c. AUV mission of Dec. 5, 1997. Squares and circles respectively mark the starting and finishing times of each of the seven legs.

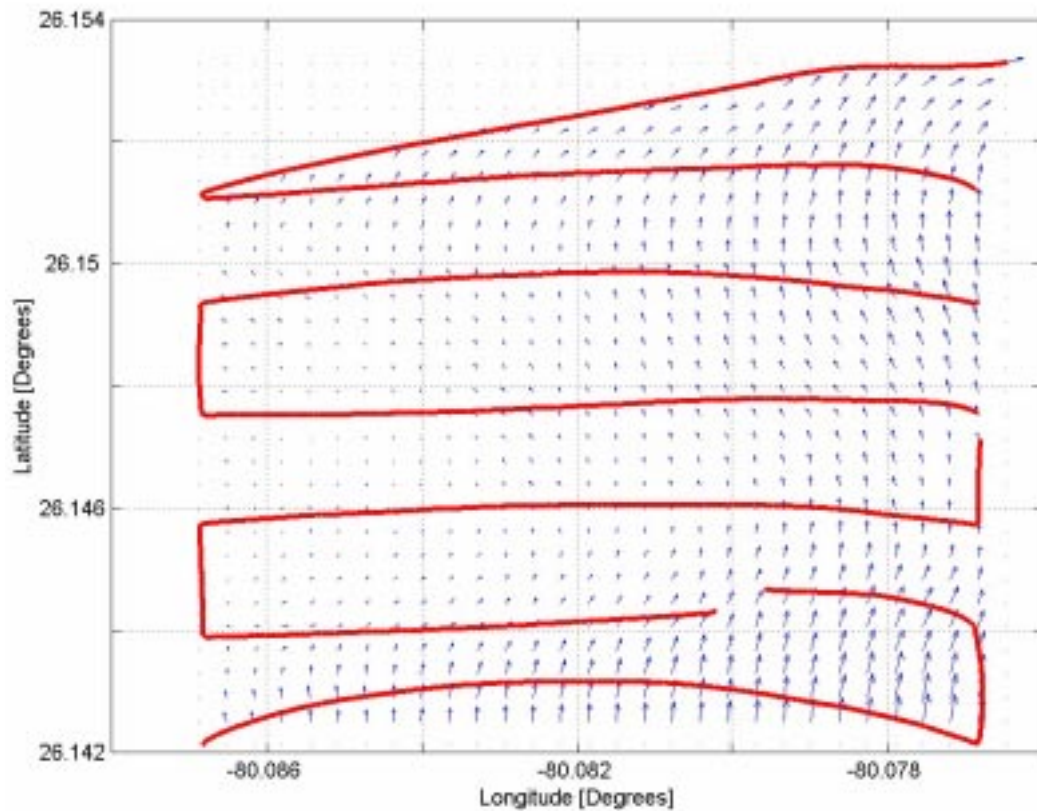


Figure 4d. AUV path and measured current at a depth of 9m on Dec. 5, 1997.

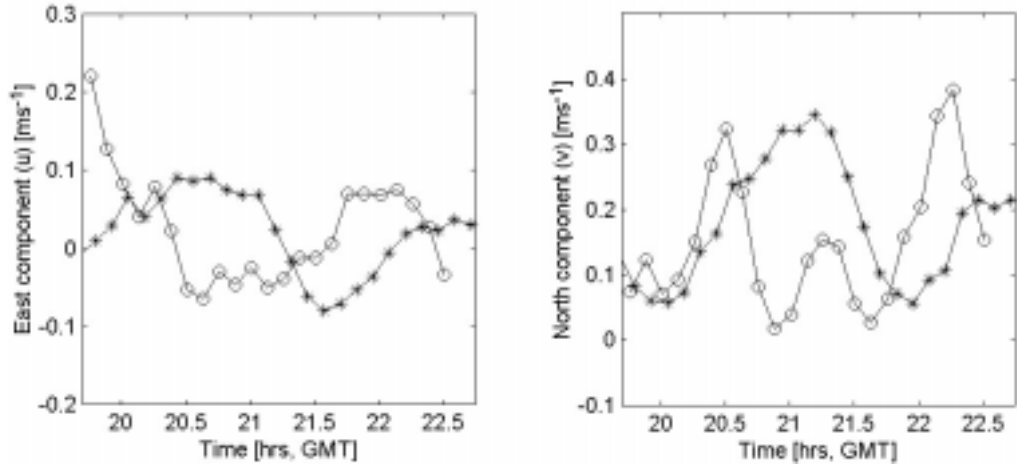


Figure 4e. Comparison between north and east components of velocity on Dec. 5, as recorded by the AUV(-o-) and by the fixed ADCP (-*-) located about 5km south of the site. Raw fixed ADCP data are shown.

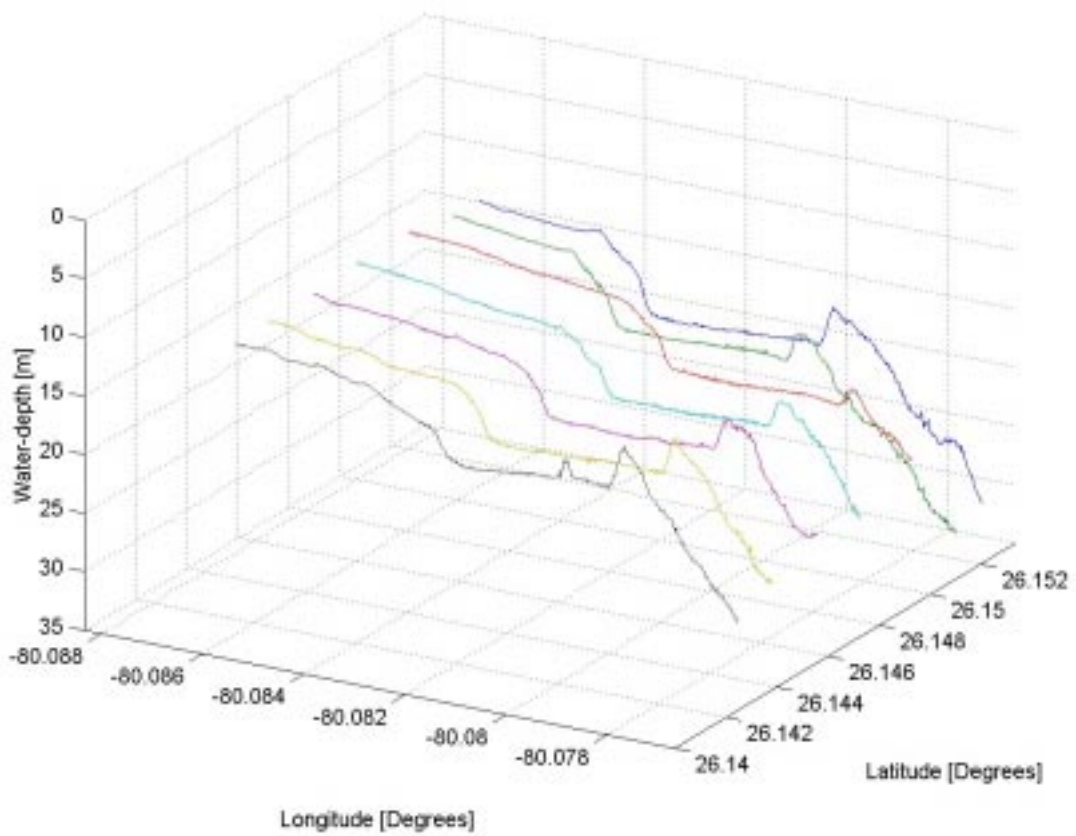


Figure 5. Instantaneous water depth during the mission of Dec. 5, 1997.

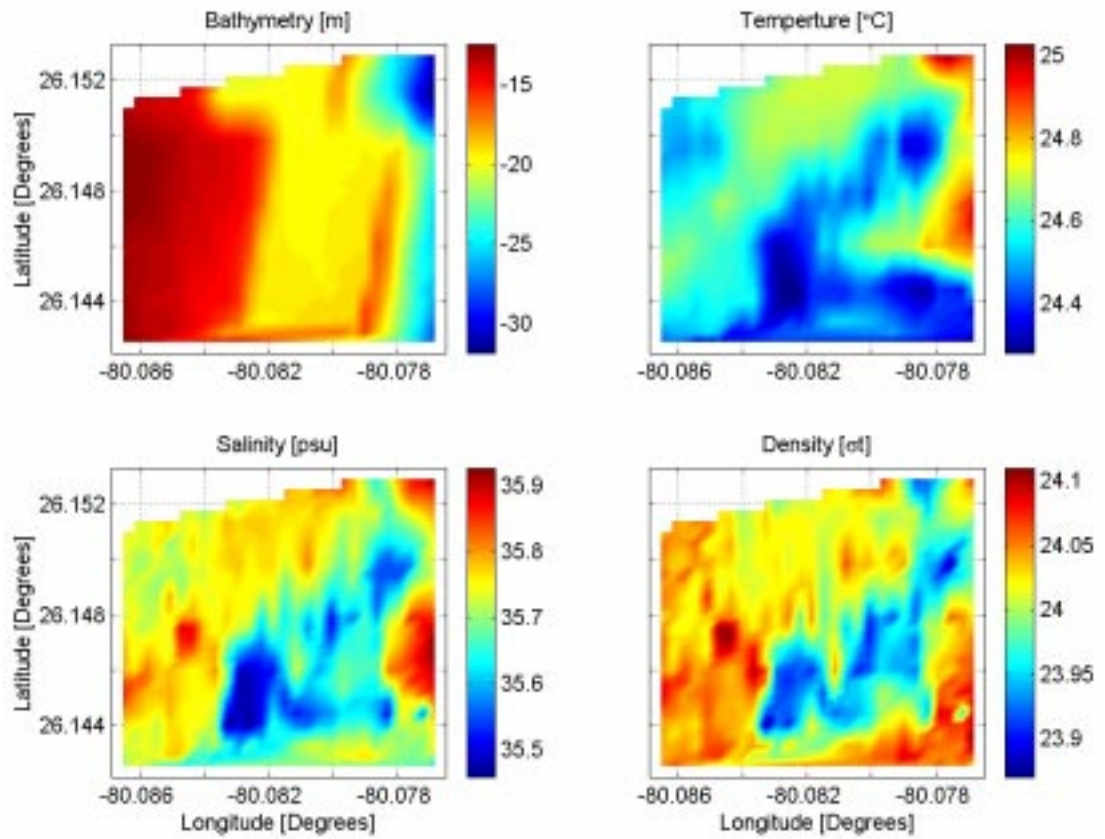


Figure 6. Regional maps of (a) bathymetry, inferred from Figure 5, (b) water temperature, (c) salinity and (d) density.

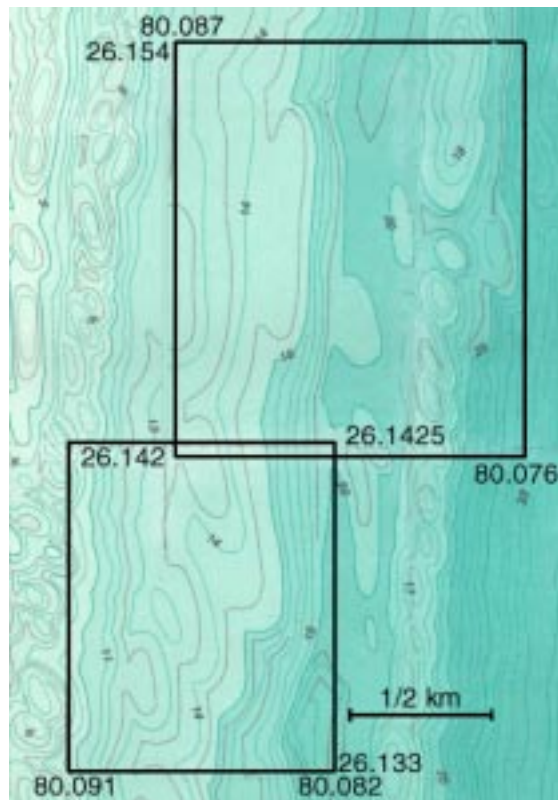


Figure 6e. Bathymetry of the two surveyed regions (boxed) according to US Geological Survey of 1962.

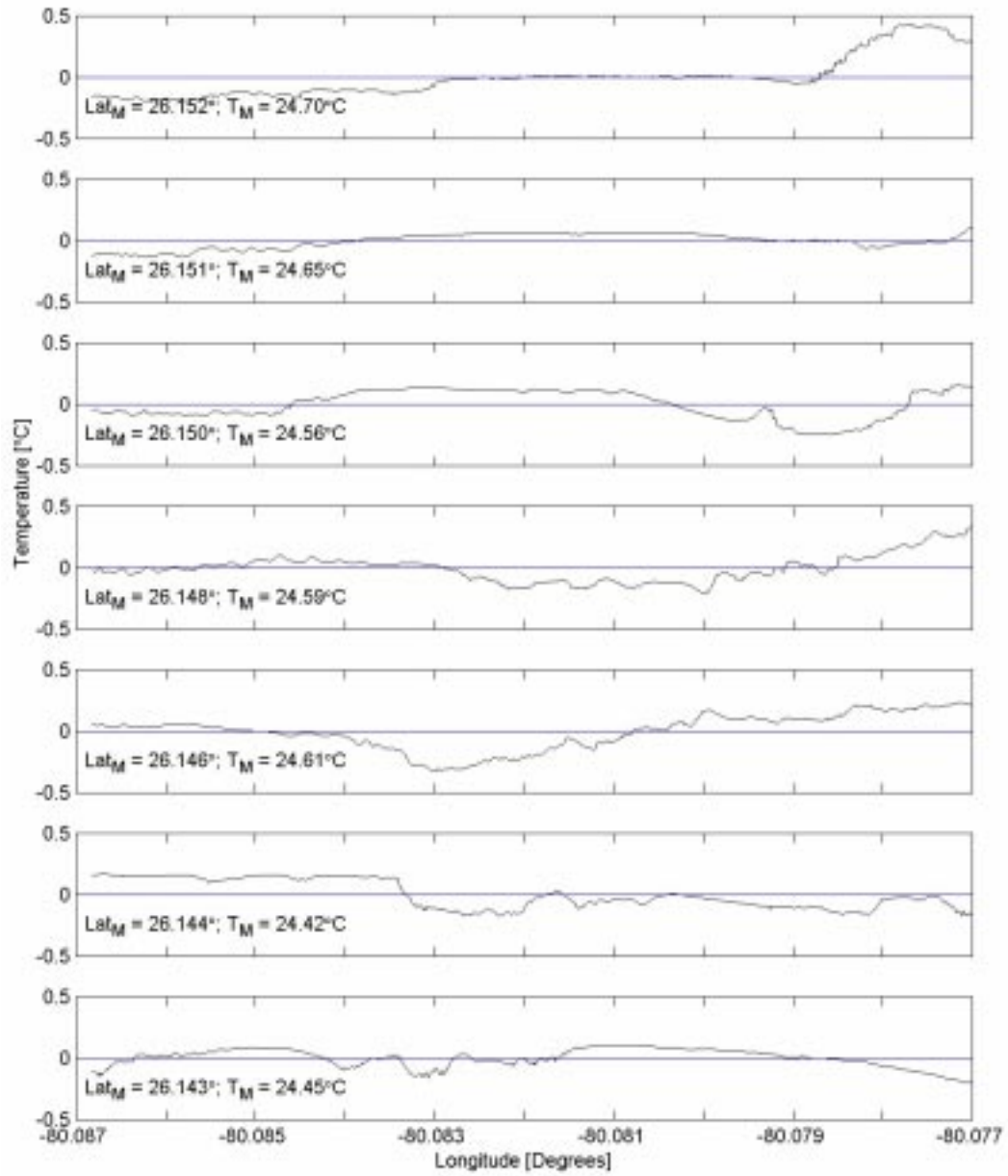


Figure 7. Temperature variations about the mean value T_M for each leg at mean latitude Lat_M plotted against instantaneous longitudinal position of AUV on 12/5/97.

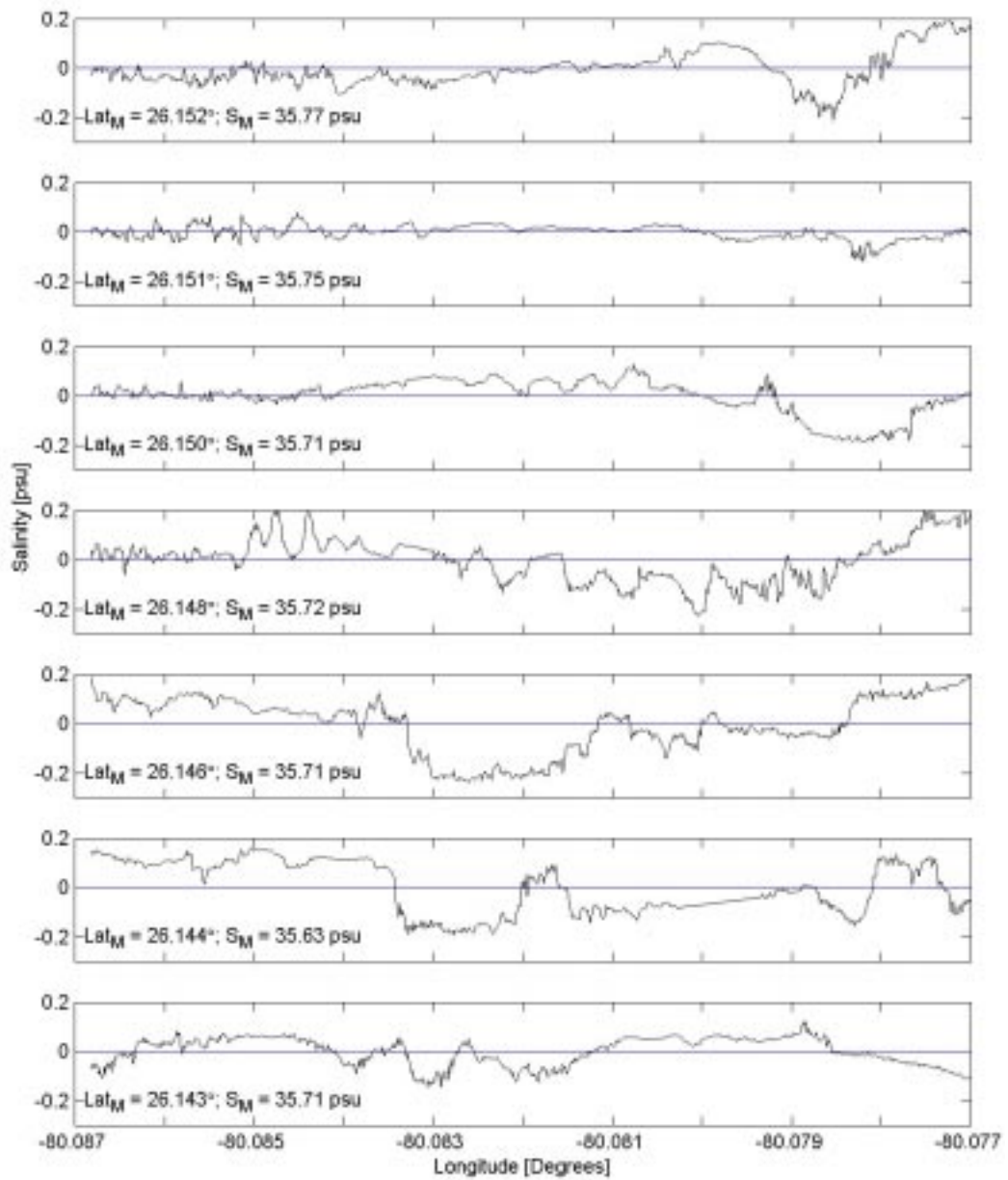


Figure 8. Salinity variations about the mean value of S_M for each leg at mean latitude Lat_M plotted against instantaneous longitudinal position of AUV on 12/5/97.

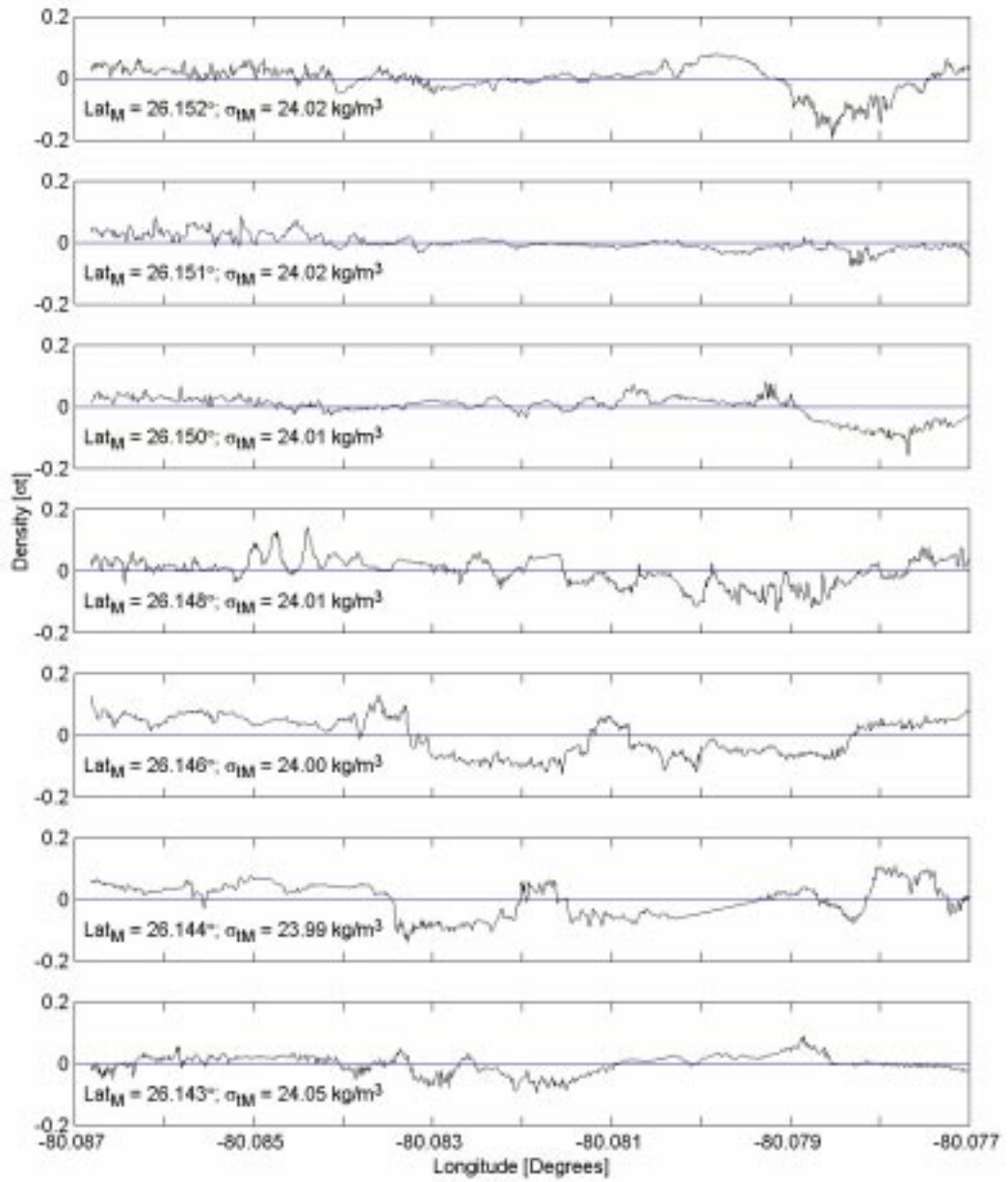


Figure 9. Density variations about the mean value of σ_M for each leg at mean latitude Lat_M plotted against instantaneous longitudinal position of AUV on 12/5/97.

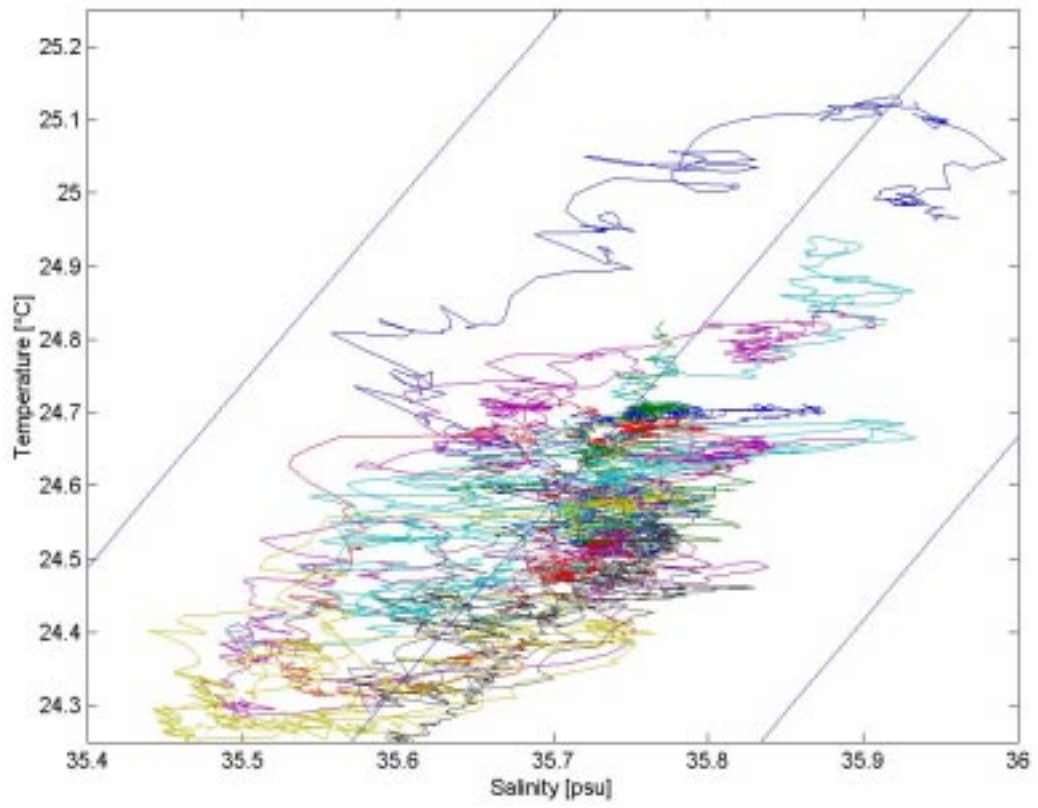


Figure 10. TS Diagram for the recorded data during the mission of 12/5/97.

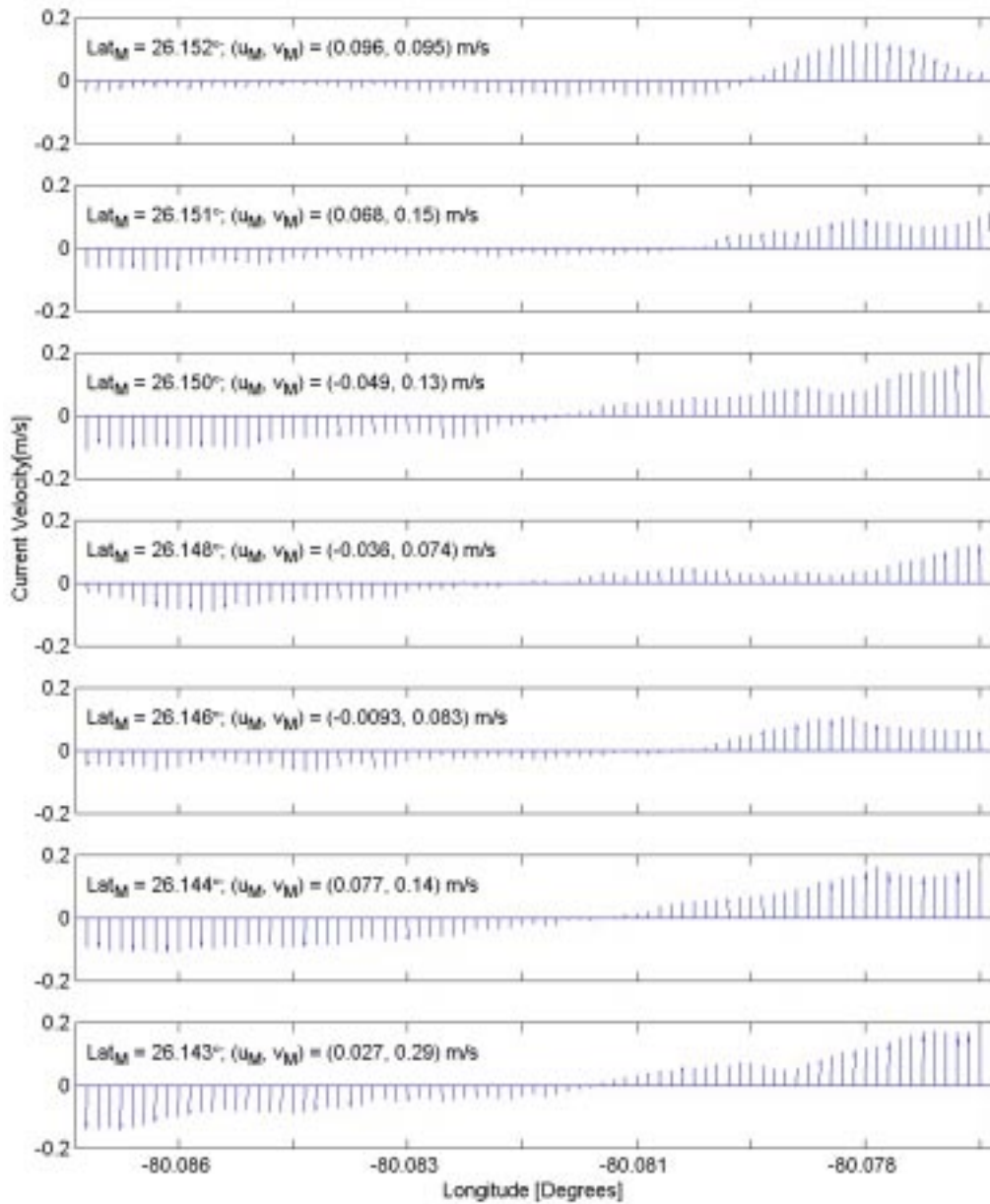


Figure 11. Current variation at 9m. depth over the seven legs about the mean value, plotted against the instantaneous longitudinal position of the AUV on 12/05/97. The magnitudes of the east, north components (u_M, v_M) of the mean current are shown in each subplot.

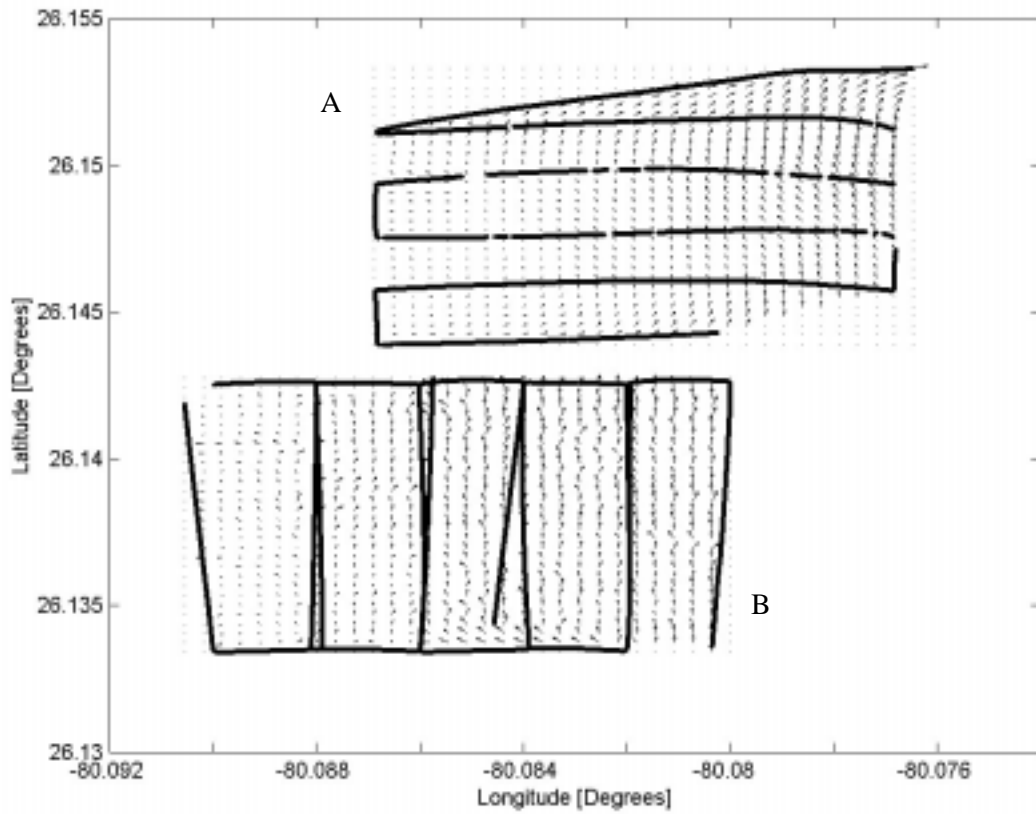


Figure 12. AUV paths and current distributions at 9m on 12/05/97 (marked A) and at 5m on 12/11/97 (marked B) mapped on latitude-longitude plane. Arrow sizes are scaled to represent speed in the range (0-31cm/s)

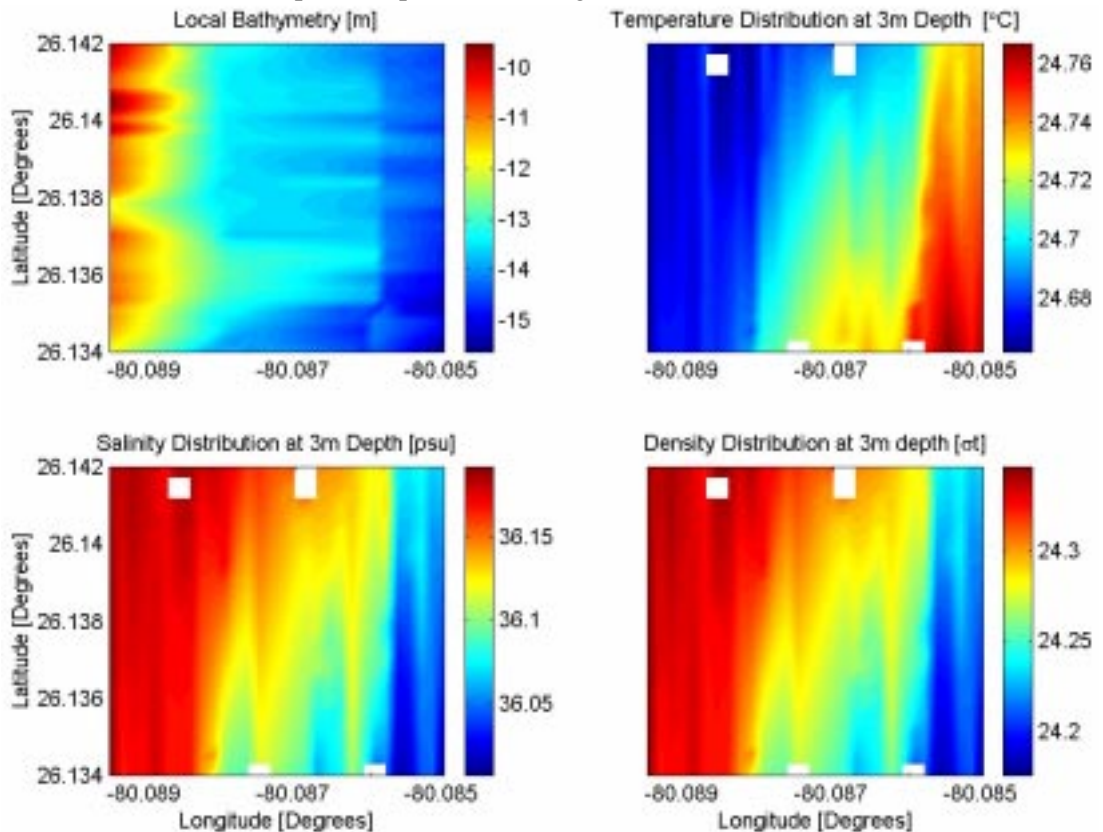


Figure 13. Regional maps of (a) bathymetry, (b) water temperature, (c) salinity and (d) density at 7m depth on 12/11/97.

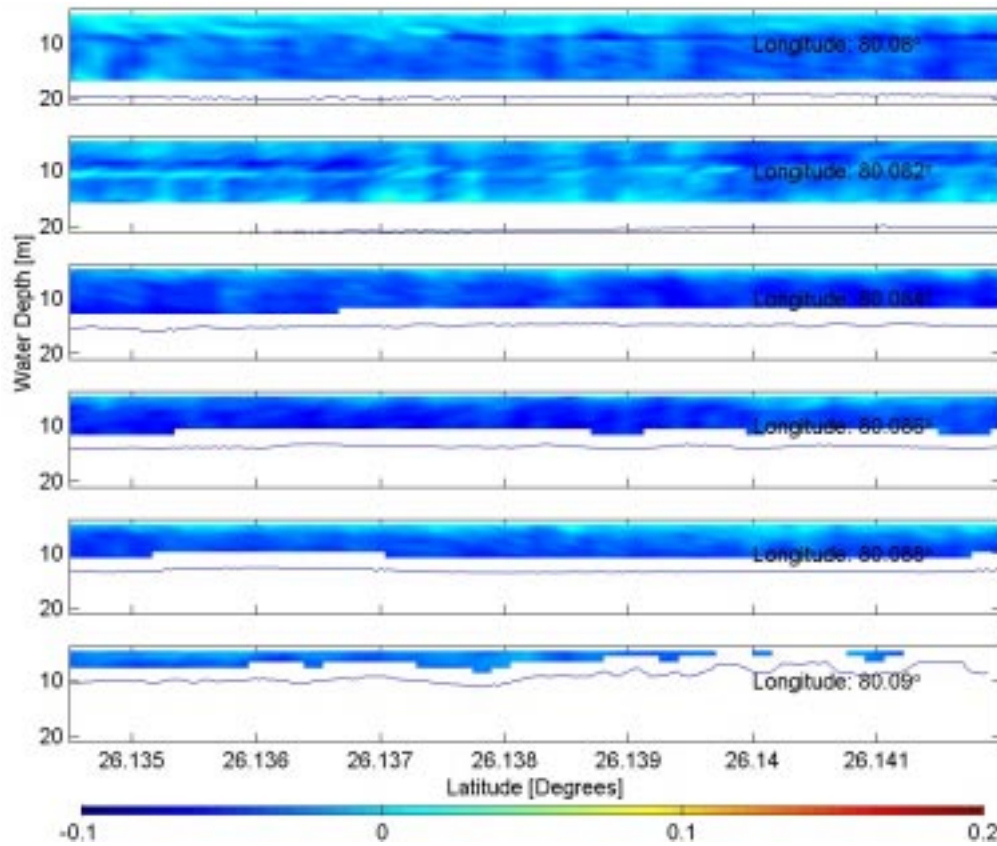


Figure 14. Variation with latitude of the (a) east (cross-shelf) (b) north (along-shelf) and (c) vertically downward component of the current profile beneath the AUV recorded during the mission of 12/11/97 at six longitudinal locations. The solid lines mark the location of the seabed.

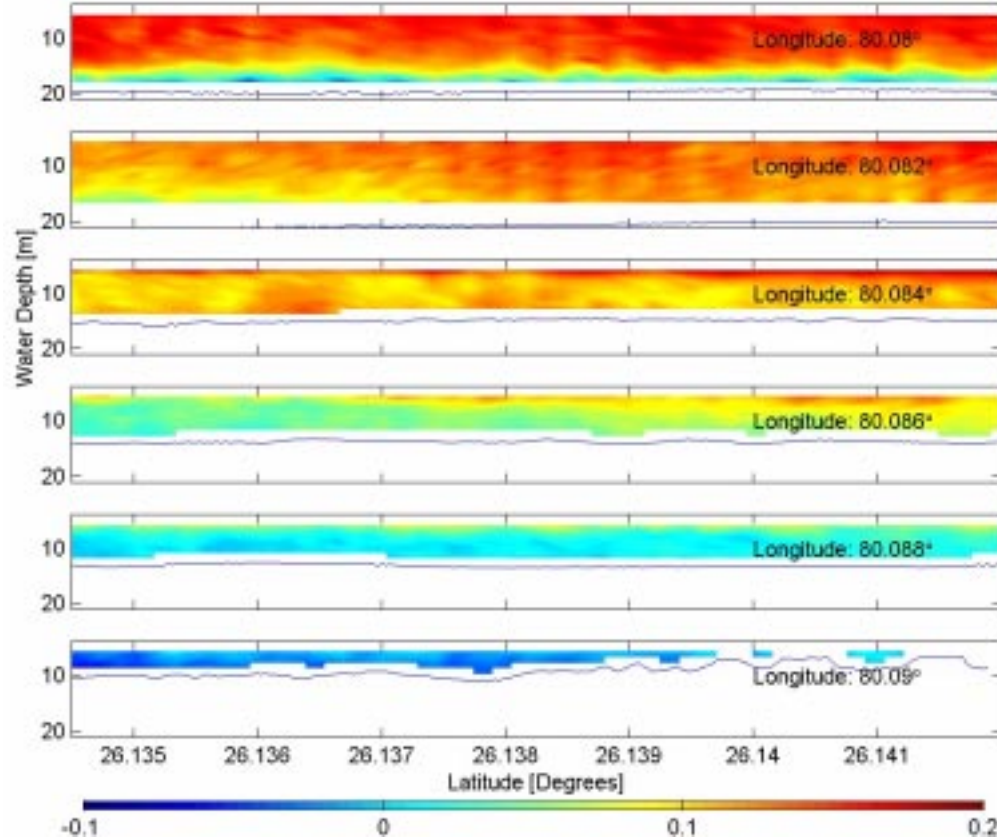


Figure 14b. See caption beneath Figure 14a.

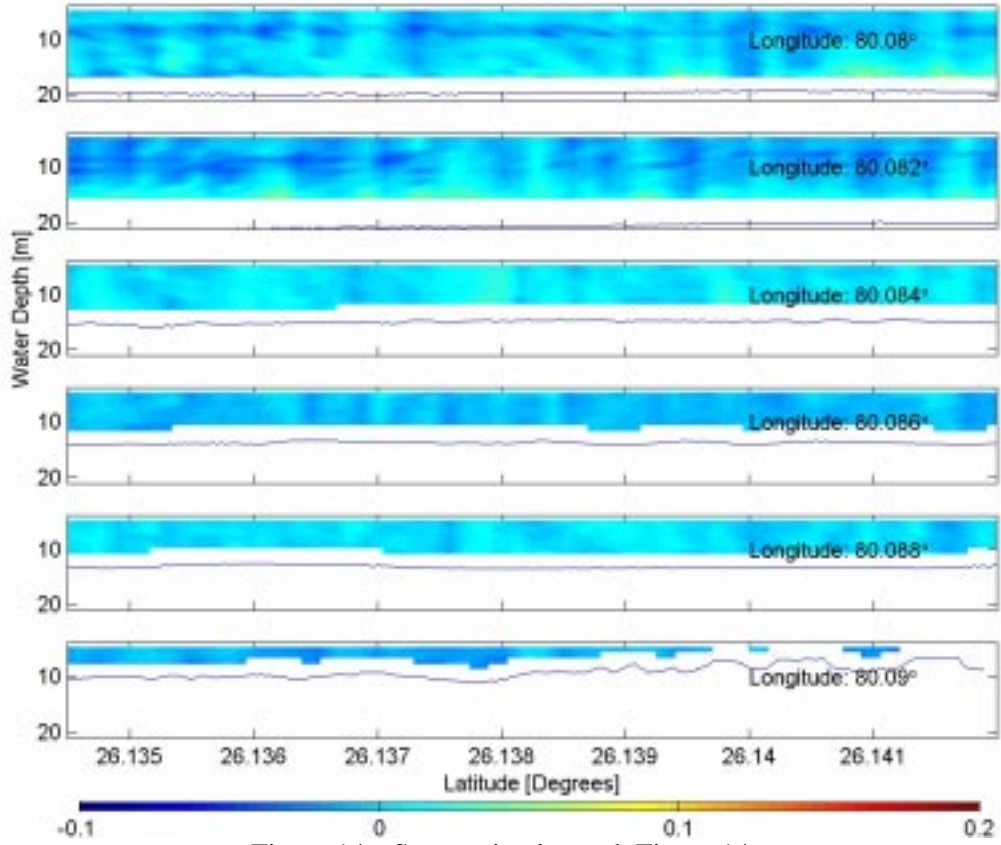


Figure 14c. See caption beneath Figure 14a.

Depth	K_1				M_2				u			v		
	u	ϕ_u	v	ϕ_v	u	ϕ_u	v	ϕ_v	σ_o^2	σ_p^2		σ_o^2	σ_p^2	
	m	cm s ⁻¹	°	cm s ⁻¹	°	cm s ⁻¹	°	cm s ⁻¹	°	cm ² s ⁻²	%	cm ² s ⁻²	%	%
4	0.4	164	5.1	158	1.9	32	6.3	-36	55	3	7	718	50	7
5	0.4	180	5.0	159	1.8	34	6.2	-35	51	3	6	730	51	7
6	0.4	-170	4.9	159	1.7	36	6.2	-35	46	2	5	731	51	7
7	0.4	-160	4.8	160	1.5	38	6.3	-34	44	2	5	724	51	7
8	0.5	-150	4.7	160	1.4	38	6.3	-34	42	2	4	711	50	7
9	0.6	-146	4.5	161	1.2	39	6.3	-33	40	2	4	697	49	7
10	0.6	-145	4.3	162	1.1	41	6.2	-32	38	2	4	677	47	7
11	0.7	-150	4.2	162	1.0	41	6.2	-32	37	1	4	656	39	6
12	0.8	-148	4.1	162	0.9	42	6.1	-31	35	1	3	633	38	6
13	0.8	-153	3.9	162	0.9	45	6.0	-31	35	1	3	607	36	6
14	0.9	-154	3.8	162	0.8	50	5.9	-30	34	1	3	576	34	6
15	1.0	-157	3.7	163	0.8	52	5.7	-29	34	1	3	544	33	6
16	0.9	-156	3.6	163	0.8	58	5.5	-29	34	1	3	508	30	6
17	0.9	-158	3.5	162	0.8	60	5.2	-28	32	1	3	454	27	6
18	0.8	-157	3.3	163	0.8	64	4.9	-28	31	1	3	403	24	6

Table 2.: Amplitudes (u,v) and relative phases (ϕ_u, ϕ_v) of the rotated diurnal (K_1) and semidiurnal (M_2) tidal components derived from a harmonic analysis of the OSCR surface currents ($z=0$) and the ADCP subsurface currents measurements at the mouth of the Port Everglades. The observed (σ_o^2) and predicted variance (σ_p^2) and the percent of explained variance by a combination of the K_1 , O_1 , M_2 , and S_2 tidal constituents are also given. Note the maximum variance region is bold faced to demonstrate the location of the core of the Florida Current. The astronomical phases at the beginning of the time series on 18 May 1994 for the K_1 and M_2 are 346° and 307° , respectively (from Shureman, 1940).